THERMAL DEVELOPMENT FOR DUCTS OF ARBITRARY CROSS-SECTIONS BY BOUNDARY-FITTED COORDINATE TRANSFORMATION METHOD

M. A. Isazadeh

Department of Chemical Engineering, University of Petroleum Industry
Ahwaz, Iran

Abstract   The non-orthogonal boundary-fitted coordinate transformation method is applied to the solution of steady three-dimensional momentum and energy equations in laminar flow to obtain temperature field and Nusselt numbers in the thermal entry region of straight ducts of different cross-sectional geometries. The conservation equations originally written in Cartesian coordinates are parabolized in the axial direction and then transformed to the non-orthogonal curvilinear coordinate system to handle arbitrary duct geometries. The transformed equations are discretized using the control-volume finite-difference approach in which the convective and diffusive terms are discretized by the upwind and central difference schemes respectively. The discretization equations are solved by a line-by-line TDMA algorithm. Numerical results of Nusselt numbers and temperature profiles are obtained for constant wall temperature boundary condition and Pr = 6.78.

Key Words   Boundary-Fitted Coordinates, Thermal Development, Arbitrary Cross-Sectional Ducts

چکیده   روش غیر متعامد در برگیرنده حدود اشکال هندسی برای حل معادلات دائمی سه بعدی ممنتوم و انرژی در جریان آرام به کار برده شده تا میدان دما و اعداد ناسلت در منطقه حرارتی ورودی مجراهای مستقیم با سطح مقطع مختلف بدست آید. معادلات بقا که در ابتدا در مختصات کارتزین نوشته شده، در جهت محوری پارابولیزه شده و سپس به سیستم مختصات غیر متعامد منحنی ـ خطی انتقال می‌یابند تا اشکال هندسی دلخواه را بگیرند. معادلات انتقال یافته با روش تفاضل های متناهی، توزیع گسسته یافته که در آن به جملات جابجایی و نفوذ به ترتیب با روش upwind و روش central difference برخورد می‌شوند. معادلاتی که توزیع گسسته یافته اند، با الگوریتم TDMA خط به خط حل می‌شوند. نتایج عددی اعداد ناسلت و پروفیل‌های دما برای شرایط مرزی دمای ثابت دیواره Pr = ٦/٧٨ بدست آورده شده است.

1. INTRODUCTION

A review of literature reveals that the majority of the studies in this area were related to rectangular and square ducts. Clark and Kays [1] obtained the fully developed theoretical and experimental Nusselt numbers and temperature profiles for laminar flow constant temperature and constant heat flux boundary conditions in rectangular ducts. Han [2] obtained an analytical solution for fully developed temperature profiles in laminar flow for rectangular ducts with two opposite walls treated as extended surfaces. Sparrow and Siegel [3] obtained the fully developed temperature profiles for constant peripheral heat flux using a variational method. Dennis et al. [4] considered the thermal entrance region problem

and obtained the analytical solution of heat transfer to the wall of a rectangular duct through which a hot viscous fluid passes in steady laminar motion. Savino and Siegel [5] analyzed the effect of unequal heat flux at adjacent walls of rectangular ducts for fully developed laminar heat transfer. Montgornery and Wibulswas [6] obtained the thermal entrance region Nusselt numbers for constant flux boundary condition in rectangular ducts with infinite wall conduction by finite difference method. Shah and London [7] collected up to 1978 of a review of the laminar flow heat transfer literature for rectangular ducts. Lyczkowski. Solbrig and Gidaspow [8] obtained a finite difference solution for laminar flow heat transfer of a flowing gas in a rectangular duct for different boundary conditions.
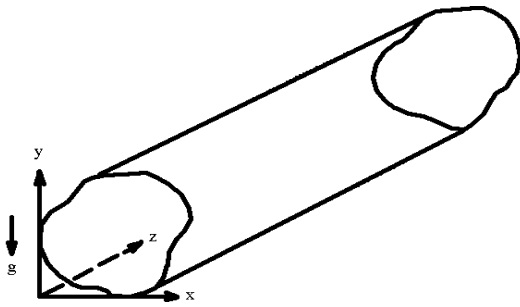
Figure 1. Arbitrary cross-sectional duct in Cartesian coordinates.

Figure 2. Grid arrangement adopted at each axial section.

Results have been obtained for several duct aspect ratios in the thermal entrance and in the fully developed regions. Neti and Eichhorn [9] presented results of a finite difference study of combined entrance region development (hydrodynamic plus thermal) in square ducts. Temperature profiles and Nusselt number variations are presented for the constant wall temperature case and Pr = 6.0. They have shown that Nusselt number values are smallest near the corners and largest on the central planes.

The objective of the present study is to develop a numerical method by non-orthogoanl boundary-fitted transformation to analyze the thermal entry region of ducts of complex geometry cross-sections [10]. Results are presented for square, triangular, trapezoidal and pentagonal ducts.

2. THE MATHEMATICAL MODELLING

The basic equations, boundary conditions and simplifying arrangements used in this study are illustrated in the following sections and Figures 1 to 6.

The Governing Equations   The strongly conservative form [11] of the steady overall continuity, momentum and energy equations are expressed as follows:

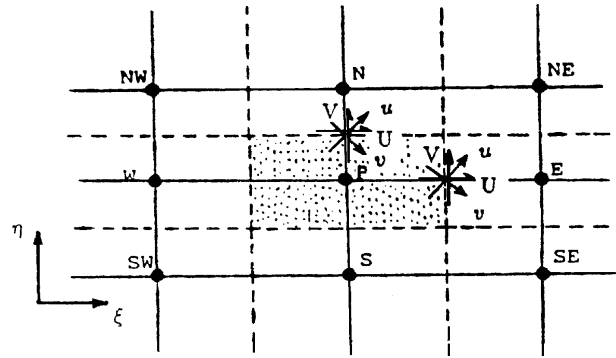**The Overall Continuity Equation**

$$(\nabla \cdot \rho v) = 0 \tag{1}$$

The Momentum Equation

$$-(\nabla \cdot \rho vv) - \nabla P - (\nabla \cdot \tau) + \rho g = 0 \tag{2}$$

The Energy Equation

$$(\nabla \cdot \rho C_p Tv) + (\nabla . q) + (\tau \nabla v) = 0 \tag{3}$$

The conservative form enhances the subsequent treatment of the equations for numerical solution. The body force i.e. the gravitational field is applied only in the "y" direction for the coordinate system selected in Figure 1. For the case where there is a variation of density with temperature in the flow field, the body force term can be modified to a buoyancy force term along with a modified definition of the pressure [12,13]. The buoyant force is the cause of a natural convection flow in the transverse direction.

The Parabolized Governing Equations in Cartesian Coordinates

The Overall Continuity Equation

$$\frac{\partial(\rho u)}{\partial x} + \frac{\partial(\rho v)}{\partial y} + \frac{\partial(\rho w)}{\partial z} = 0 \tag{4}$$

The Momentum Equations
x-component

$$\frac{\partial}{\partial x}(\rho u^2) + \frac{\partial}{\partial y}(\rho vu) + \frac{\partial}{\partial z}(\rho wu) =$$
$$-\frac{\partial P}{\partial x} - (\frac{\partial \tau_{xx}}{\partial x} + \frac{\partial \tau_{yx}}{\partial y}) \tag{5}$$
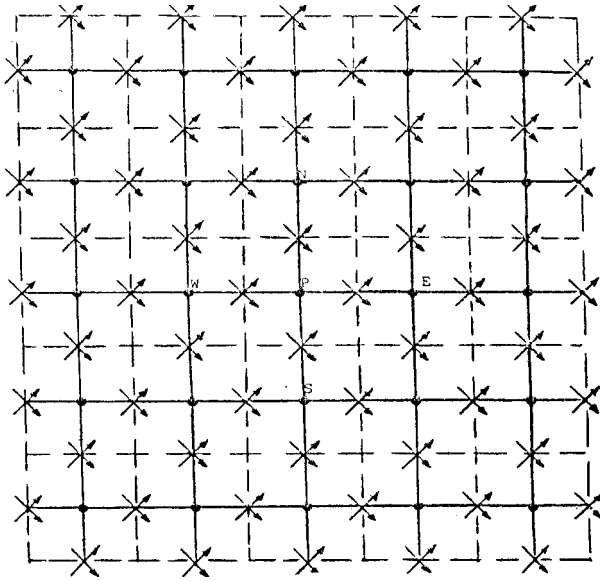
Figure 3. .Physical velocities over the completely computational domain.

y-component

$$\frac{\partial}{\partial x}(puv) + \frac{\partial}{\partial y}(pv^2) + \frac{\partial}{\partial z}(pwv) =$$
$$-\frac{\partial P}{\partial y} - (\frac{\partial \tau_{xy}}{\partial x} + \frac{\partial \tau_{yy}}{\partial y}) - (\rho - \rho_a)g \qquad (6)$$

z-component

$$\frac{\partial}{\partial x}(\rho uw) + \frac{\partial}{\partial y}(pvw) + \frac{\partial}{\partial z}(pw^2) =$$
$$-\frac{d\bar{P}}{dz} - (\frac{\partial \tau_{xz}}{\partial x} + \frac{\partial \tau_{yz}}{\partial y}) \qquad (7)$$

The Energy Equation

$$\frac{\partial}{\partial x}(\rho C_P Tu) + \frac{\partial}{\partial y}(\rho C_P Tv) + \frac{\partial}{\partial z}(\rho C_P Tw) =$$
$$\frac{\partial}{\partial x}(k\frac{\partial T}{\partial x}) + \frac{\partial}{\partial y}(k\frac{\partial T}{\partial y}) + \mu..\Phi_v \qquad (8)$$

The pressure, P in the above equations is dynamic pressure due to the introduction of buoyancy terms in the "y" momentum equation. In cases of negligible buoyancy effect, P would be the total pressure defined as hydrostatic plus dynamic pressures.

The Boundary Conditions

Inlet ($@_z = 0$)

1. **Axial Velocity** A uniform entrance velocity profile is specified at inlet:

$$w = w_{inlet} \qquad (9)$$

2. **Transverse Velocities** It is assumed that there is no secondary flow at inlet:

$$u = 0, v = 0 \qquad (10)$$

3. **Temperature** A uniform temperature profile is assumed at inlet:

$$T = T_{wall} \qquad (11)$$

Walls of the Duct

1. **Axial Velocity** No slip-condition is assumed on the walls of the duct:

$$w = 0 \qquad (12)$$

2. **Transverse Velocities**

$$u = 0, v = 0 \qquad (13)$$

3. **Temperature** For a constant wall temperature:

$$T = T_{wall} \qquad (14)$$

Outflow Conditions For the parabolized governing equations used here no downstream boundary conditions are required.
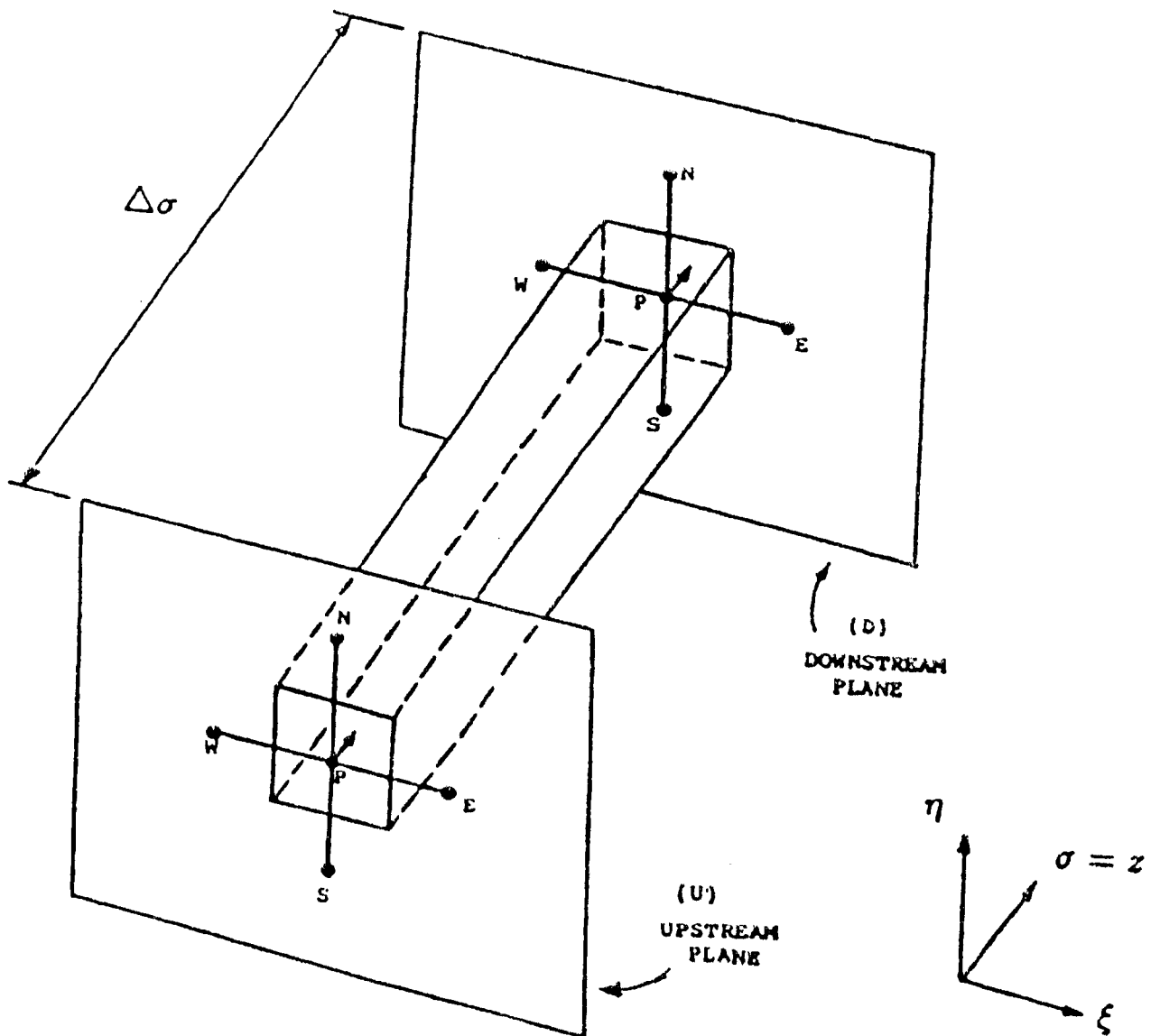
Figure 4. Three-dimensional control volume in transformed-plane.

3. THE NUMERICAL METHOD OF SOLUTION

The Boundary-Fitted Method The development of the boundary-fitted method brought about the coordinate transformation of the physical domain, such as Cartesian coordinates to the curvilinear coordinates so that all the boundaries match the coordinate lines in the new system and the need to interpolate the boundary conditions as practiced before is eliminated [14,15]. The curvilinear coordinate system may be either orthogonal or non-orthogonal in the sense of the mesh generated over the physical-domain. In this study the non-orthogonal method is applied to the solution of the present three-

dimensional problem arbitrary cross-sectional ducts.

Numerical Grid Generation   This is necessary to determine the location of the coordinate lines in the interior of the physical domain. A coordinate line is specified as being coincident with each boundary line segment while the other coordinate varies monotonically along that line. A method of generating the general boundary-fitted coordinate system is to let the curvilinear coordinates to be the solutions of an elliptic partial differential system in the physical plane, with Dirichlet boundary conditions on all the boundaries.

Transformation of Governing PDE's   It is necessary to transform the partial-differential equations under consideration into the new coordinate variables before being discretized. In general, the transformation operation generates additional terms in the governing equations so that these equations become more complicated upon transformation. The physical Cartesian velocities tire retained as the dependent variables in transformation, however, contravariant velocity components also take part in the structure of the transformed equations. The transformed equations and boundary conditions are as follows:

The Overall Continuity Equation

$$\frac{\partial(\rho U)}{\partial \xi} + \frac{\partial(\rho V)}{\partial \eta} + \frac{\partial(\rho W)}{\partial \sigma} = 0 \qquad (15)$$

The Momentum Equations

x-component

$$\frac{\partial}{\partial \xi}(\rho u U) + \frac{\partial}{\partial \eta}(\rho u V) + \frac{\partial}{\partial \sigma}(\rho u W) =$$

$$-\frac{\partial}{\partial \xi}\left[y_\eta(\hat{\tau}_{xx}) - x_\eta(\hat{\tau}_{yx})\right]$$

$$-\frac{\partial}{\partial \eta}\left[x_\xi(\hat{\tau}_{yx}) - y_\xi(\hat{\tau}_{xx})\right] - \left[y_\eta P_\xi - y_\xi P_\eta\right]$$

$$(16)$$

y-component

$$\frac{\partial}{\partial \xi}(\rho v U) + \frac{\partial}{\partial \eta}(\rho v V) + \frac{\partial}{\partial \sigma}(\rho v W) =$$

$$-\frac{\partial}{\partial \xi}\left[y_\eta(\hat{\tau}_{xy}) - x_\eta(\hat{\tau}_{yy})\right]$$

$$-\frac{\partial}{\partial \eta}\left[x_\xi(\hat{\tau}_{yy}) - y_\xi(\hat{\tau}_{xy})\right] - \left[x_\xi P_\eta - x_\eta P_\xi\right]$$

$$-J(\rho - \rho_a)g$$

$$(17)$$

z-component

$$\frac{\partial}{\partial \xi}(\rho w U) + \frac{\partial}{\partial \eta}(\rho w V) + \frac{\partial}{\partial \sigma}(\rho w W) =$$

$$-\frac{\partial}{\partial \xi}\left[y_\eta(\hat{\tau}_{xz}) - x_\eta(\hat{\tau}_{yz})\right]$$

$$-\frac{\partial}{\partial \eta}\left[x_\xi(\hat{\tau}_{yz}) - y_\xi(\hat{\tau}_{xz})\right] - J\frac{d\overline{P}}{d\sigma}$$

$$-J(\rho - \rho_a)g$$

$$(18)$$

The Energy Equation

$$\frac{\partial}{\partial \xi}(\rho C_P T U) + \frac{\partial}{\partial \eta}(\rho C_P T V) + \frac{\partial}{\partial z}(\rho C_P T W) =$$

$$\frac{\partial}{\partial \xi}\left[\frac{\alpha}{J}kT_\xi - \frac{\beta}{J}kT_\eta\right] + \frac{\partial}{\partial \eta}\left[\frac{\gamma}{J}kT_\eta - \frac{\beta}{J}kT_\xi\right] + J\hat{\mu}\hat{\Phi}_v$$

$$(19)$$

The Boundary Conditions

Inlet (@$_z$ = 0)
1.   Axial Velocity

$$w(\xi,\eta) = w_{inlet} \qquad (20)$$

2.   Transverse Velocities

$$u(\xi,\eta) = 0, \ v(\xi,\eta) = 0 \qquad (21)$$

3. Temperature

$$T(\xi, \eta) = T_{inlet} \tag{22}$$

Walls of the Duct

1. Axial Velocity

$$w(\xi, \eta) = w_{inlet} \quad \begin{array}{l} 1 \leq \xi \leq L_1 \text{ for } \eta = 1,..., M_1 \\ 1 \leq \eta \leq M_1 \text{ for } \xi = 1,..., L_1 \end{array} \tag{23}$$

2. Transverse Velocities

$$u(\xi, \eta) = 0, \ v(\xi, \eta) = 0 \quad \begin{array}{l} 1 \leq \xi \leq L_1 \text{ for } \eta = 1,..., M_1 \\ 1 \leq \eta \leq M_1 \text{ for } \xi = 1,..., L_1 \end{array} \tag{24}$$

3. Temperature

$$T(\xi, \eta) = T_{wall} \quad \begin{array}{l} 1 \leq \xi \leq L_1 \text{ for } \eta = 1,..., M_1 \\ 1 \leq \eta \leq M_1 \text{ for } \xi = 1,..., L_1 \end{array} \tag{25}$$

Note: transformation parameters:

$$\begin{aligned}
\alpha &= x_\eta^2 + y_\eta^2 \\
\beta &= x_\xi x_\eta + y_\xi y_\eta \quad &U &= y_\eta u - x_\eta v \\
\gamma &= x_\xi^2 + y_\xi^2 \quad &V &= x_\xi v - y_\xi u \\
J &= x_\xi y_\eta - x_\eta y_\xi \quad &W &= Jw
\end{aligned} \tag{26}$$

Discretization of Transformed Equations

For a non-orthogonal grid system, the best grid configuration is a modified classical staggered-grid in which both components of "if and "v" velocities are used coincidentally at the same location with the contravariant-velocities normal and parallel to the faces of the cell (Figure 2). Physical velocities over the whole computational domain is shown in Figure 3. A three-dimensional control volume is shown in Figure 4.

The transformed governing equations are discretized using the method known as the "control-volume" approach [16,17]. The upwind difference scheme is used for discretization of convective terms and the central difference scheme is used for discretization of diffusion terms. The discretization equations are algebraic equations and are solved by a line-by-line tridiagonal matrix (TDMA) algorithm. For the proper location of the control-volume faces, the B-type grid [17] is employed here. The pressure-velocity coupling in the transverse direction is handled by the SIMPLER algorithm [17] after being modified for the non-orthogonal coordinate system. The method adopted in this work to handle the pressure-velocity coupling in the axial direction is that of Raithby and Schneider [18].

Solution Procedure   This work demonstrates the suitability of the numerical model and the solution procedure applied to 3D parabolized momentum and energy equations in straight ducts of arbitrary but uniform cross-sections. A review of some of the related developments in the numerical methods for the solution of conservation equations reveals the elegant features of the numerical procedure applied to this work. In general, coupling between the momentum and mass conservation equations is often the major cause of the slow convergence of the iterative solution methods. Caretto et al. [19] applied a numerical method to the solution of the momentum equations, which involved an implicit simultaneous solution of coupled nonlinear difference equations without linearization or decoupling. The solution procedure was, however, a point-by-point iterative method due to which slow convergence is inevitable. The method of Patankar and Spalding [16] involved linearization and decoupling of the equations. In their method, the non-linear terms (the product terms) of the momentum equations are handled by setting the value of velocities in these terms the same as their values at the previous axial step.

The axial momentum equation is treated separately from the transverse momentum equations, which are decoupled by assuming a pressure-field in the transverse direction. In the computations of transverse velocities, corrections are made for the tentative transverse velocities and pressure field by iteratively solving a Poisson like equation for the pressure-correction. The method proposed by Briley [20] requires two Poisson like equations to be solved, one for a velocity potential for velocity corrections and the other for the pressure field. The method of Patankar and Spalding [16] developed later brought about the

Square   Equilateral-triangular   Trapezoidal   Pentagonal

Figure 5. The selected geometries in the physical domain.

21×21 B-type grid for square duct   21×21 B-type grid for triangle duct

21×21 B-type grid for trapezoidal duct   21×21 B-type grid for pentagonal duct
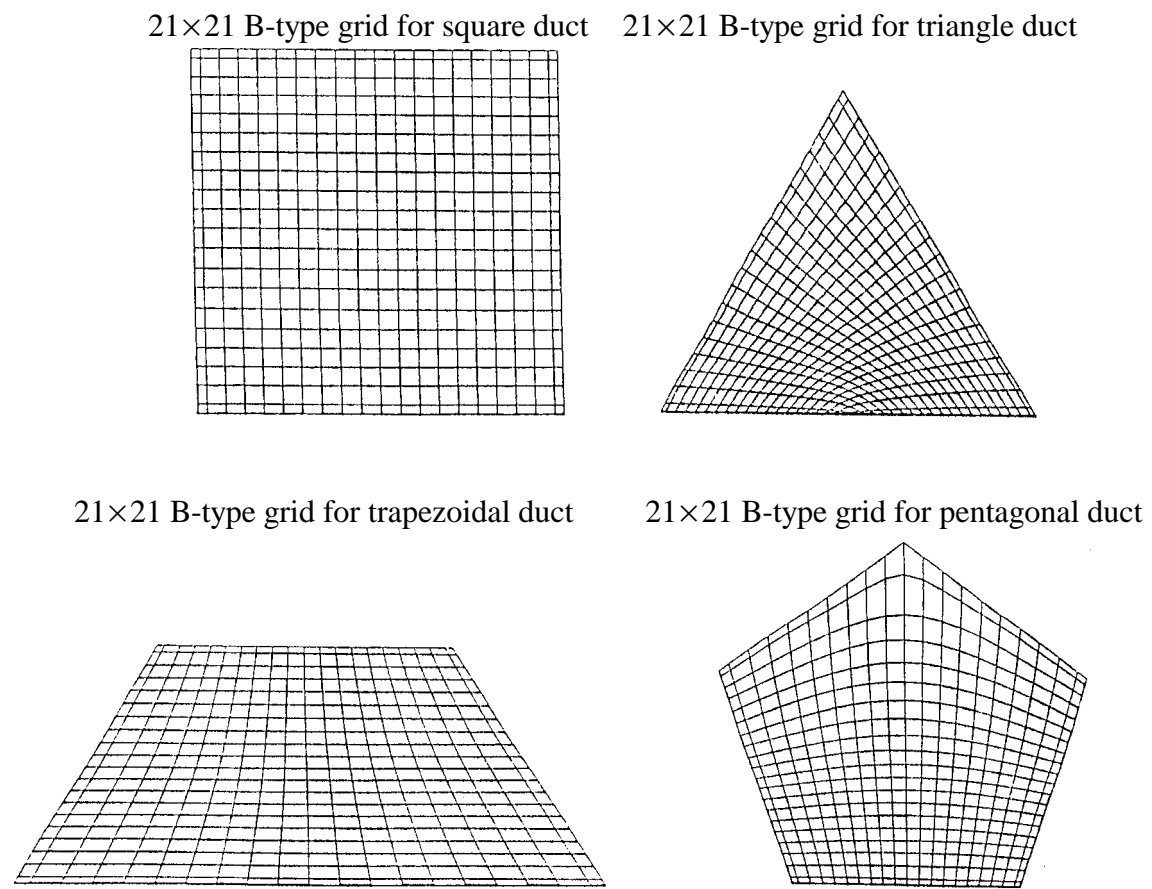
Figure 6. The selected geometries in the physical domain.

SIMPLE and SIMPLER algorithms [17]. The SIMPLE and SIMPLER algorithms have been already applied to solve problems using the non-orthogonal boundary fitted coordinate transformation system. Some of these works are worthy to mention here. Hadjisophocleous et al. [21], Shyy et

al. [22] and Braaten et al. [23] employed the SIMPLE algorithm in their analysis for non-orthogonal systems. Maliska [24] applied a mixed scheme comprising of SIMPLE and SIMPLER algorithms.

The use of nonorthogonal coordinates versus orthogonal system has the advantage of getting rid of the generation of orthogonal grids at certain locations, which are difficult or impossible to make. The staggered grid employed in this work uses both of the u and v velocity components at each velocity locations. This grid arrangement together with the numerical scheme in which both of the physical Cartesian and contravariant velocities are involved, have led the finite difference equations to converge faster without numerical instabilities. Besides, a combination of upwind difference scheme for the convective terms and central difference scheme for the diffusive terms, which is employed in this work, provided satisfactory results.

4. RESULTS AND DISCUSSION

The numerical results of heat transfer analysis for constant wall temperature and $P_{r} = 6.78$ are shown in Figures 7 to 8 and Tables 6 and 7. A general-purpose computer program in Fortran developed by the author was employed to obtain the present results. The specific geometries selected for the present analysis are as flows:

- square duct,
- equilateral triangular duct,
- trapezoidal duct (acute-angle = $60°$, one side twice the other),
- pentagonal duct (each angle = $108°$). These geometries are shown in Figure 5.

The grids are shown in Figure 6. All the above ducts were selected on the basis of the same equivalent diameter. Consequently, the same value of relaxation factor was applied to all geometries corresponding to each discretization equation. It is believed that this scheme is valid if the geometries selected do not involve oddity. For a pictorial representation of this concept, one may refer to Bejan [25] for a scale drawing of the duct sizes for

some geometry. Other than the ducts mentioned above, circular and rectangular ducts (of two aspect ratios: 2/1 and 3/2) were also examined for validation of the model and the computer code.

The problem was solved for an axial step size of 0.276 m for which 250 marching stations were required in the axial direction to reach to the converged solution. For the sake of numerical accuracy and computational economy the mesh size selected was 21 x 21 over the transversed plane. The memory requirement for computations was 2720 K and the typical CPU time was about 26 minutes for one run on IBM ESA9000 machine (mainframe). The computations were performed for fully developed velocity and developing temperature profiles. Referring to Kays et al. [26] the results obtained in this analysis are well suited for the simultaneously developing velocity and temperature profiles for the respective Prandtl number. The buoyancy effect in this study is negligible due to the close temperatures selected for the fluid at inlet and at wall. About 5 iterations were required to obtain converged solution over each transversed plane. The convergence criteria were set on the residual values defined as follows:

i. the residual of the energy equation, that is, the remainder of this equation when the results are substituted for the enthalpy into this equation. In general $R = \sum a_{nb}\varphi_{nb} + b - a_{P}\varphi_{P}$ and R will be zero when the discretization equation is satisfied [17].
ii. the residual of enthalpy values, that is, the difference in enthalpy values between two successive iterations.

Table 1 shows the residual values of energy equation and enthalpy values at the converged solution.

The local Nusselt number for constant temperature wall boundary conditions, is expressed in terms of the fluid bulk-temperature-gradient along the flow path length by

$$\text{Nu}_{z,T} = -\frac{1}{4\theta_{b}}\frac{d\theta_{b}}{dZ^{**}} \qquad (27)$$

Refer to the Appendix for derivation.
The logarithmic mean Nusselt number for constant

TABLE 1. Residual Values.

Geometry	Energy-equation Residual	Enthalpy Residual
Square	0.303×10^{-7}	-0.275×10^{-4}
Triangular	0.160×10^{-6}	-0.270×10^{-4}
Trapezoidal	0.533×10^{-7}	-0.270×10^{-4}
Pentagonal	0.694×10^{-7}	-0.385×10^{-4}
Rectangular (2/1)	0.224×10^{-7}	-0.357×10^{-4}
Rectangular (3/2)	0.262×10^{-7}	-0.315×10^{-4}
Circulare	0.105×10^{-6}	-0.501×10^{-4}

wall temperature boundary condition is expressed by:

$$Nu_{m,T} = \frac{1}{4Z^{**}} \ln\left(\frac{1}{\theta_b}\right) \qquad (28)$$

which is obtained from Equation 27 by integration.

The thermal entry length is analyzed in terms of the dimensionless bulk and centerline temperatures in Figure 7(a, b) and Figure 8(a, b) for square, triangular, trapezoidal and pentagonal ducts. Bulk temperature is the mean temperature over the section and centerline temperate is the mean temperature over the centerline. The thermal entry length obtained in this study for square ducts is

TABLE 2. Thermal Entry Length and Limiting Nu_T Results.

Geometry	Z^{**} = thermal entry length	Limiting Nu_T	$RT1 = \dfrac{T_{Unit} - T_{Inlet}}{T_{Wall} - T_{Inlet}}$	$RT2 = \dfrac{TCL - T_{Inlet}}{T_{Wall} - T_{Inlet}}$
Square	0.381	2.980	0.993	0.986
Triangular	0.397	2.598	0.993	0.986
Trapezoidal	0.382	2.972	0.993	0.986
Pentagonal	0.339	3.098	0.993	0.986
for comparison:				
Rectangular (2/1)	0.341	3.363	0.993	0.986
Rectangular (3/2)	0.366	3.118	0.993	0.986
Circulare	0.317	3.603	0.993	0.986

TABLE 3. Comparison of Limiting Nusselt Numbers.

	Square	Rectangular (2/1)	Rectangular (3/2)	Equilateral Triangular	Circular
Clark and Kays	2.890	3.390	-	-	-
Dennis et al.	2.980	3.390	3.120	-	-
Shah and London	2.976	3.391	3.117	-	-
Schmidt	2.970	3.383	3.121	-	-
Javeri	2.981	3.393	-	-	-
Lyczkowski et al.	2.975	3.395	3.117	-	-
Kays and Crawford	2.980	3.390	-	2.350	3.658
Wibulswas	-	-	-	2.570	-
This Study	2.980	3.363	3.118	2.598	3.603

TABLE 4. Comparison of Nusselt Number: $Nu_{z,T}$ Variation for Square Ducts.

Chandrupatla		Present Analysis	
G_z	$Nu_{z,T}$	G_z	$Nu_{z,T}$
0	2.975	0	2.980
40	3.432	37	3.204
50	3.611	50	3.527
80	4.084	75	4.104
100	4.357	100	4.635
133.3	4.755	127	4.845
200	5.412	190	5.808

TABLE 5. Comparison of Nusselt Number: $Nu_{m,T}$ Variation for Square Ducts.

Chandrupatla		Present Analysis	
G_z	$Nu_{z,T}$	G_z	$Nu_{z,T}$
0	2.975	0	2.980
40	4.841	37	4.878
50	5.173	50	5.441
80	5.989	75	6.386
100	6.435	100	7.186
133.3	7.068	127	8.084
200	8.084	190	9.612

$Z^{**} = 0.381$ which is close to the value obtained by Neti et al. [9], $Z^{**} = 0.352$. The value in this study is corresponding, however, to the dimensionless bulk and centerline temperatures of 0.993 and 0.986 respectively while the values obtained by Neti et al. [9] are that of 0.988 and 0.979 respectively. The temperature is nondimensionalized here with the difference between the fluid wall temperature and the fluid temperature at the duct entrance. The results for the limiting Nusselt numbers are indicated in Table 2 for all geometries under consideration. The limiting Nusselt numbers (Nu_T) for square, rectangular, triangular and circular ducts obtained in this study are compared with the analytical and numerical results of other investigators in Table 3. These results confirm the validity of the model and computer code in this study.

The results of central plane thermal development are shown in Figures 9(a, b) and 10(a, b) for square, triangular, trapezoidal and pentagonal ducts in terms of the dimensionless temperature profiles. The temperature is nondimensionalized here with the difference between the uniform wall temperature and the bulk fluid temperature. Temperature profiles are shown at three different axial positions. The peak value of RT for triangular and pentagonal ducts tends towards the corner of the ducts on the central plane. This is due to zero friction at corners due to which the peak value of velocity profile on the central plane tends closer to

the corner and induces temperature accordingly.

The results obtained for square ducts for Newtonian fluids ($Nu_{z,T}$, $Nu_{m,T}$) are compared with the numerical solutions of Chandrupatla & Sastri [27] in Tables 4 and 5. There is a close agreement between their solutions and the present results for $Nu_{z,T}$ but there are some differences between $Nu_{m,T}$ values. The results obtained by Chandrupatla and Sastri [27] are with no secondary flow and no viscous dissipation effects. Also, the effect t of variation of Prandtl number is ignored in their analysis and no value is mentioned for the Prandtl number corresponding to their results. It is believed that, the differences existing in the results of $Nu_{m,T}$ as observed in Table 5 are mainly due to the difference in the values of Prandtl numbers. Chandrupatla and Sastri [27] ignores the effect of Prandtl number on $Nu_{m,T}$ by reasoning that it is included in the relevant $\dfrac{Pr}{(X/4)}$ term. However, $Nu_{m,T}$ is affected by Pr through the effect θ_b according to the following relations:

$$Nu_{m,T} = \frac{Pr}{X}\ln\frac{1}{\theta_b} = \frac{1}{4}\frac{Pr}{(X/4)}\ln\left(\frac{1}{\theta_b}\right) \qquad (29)$$
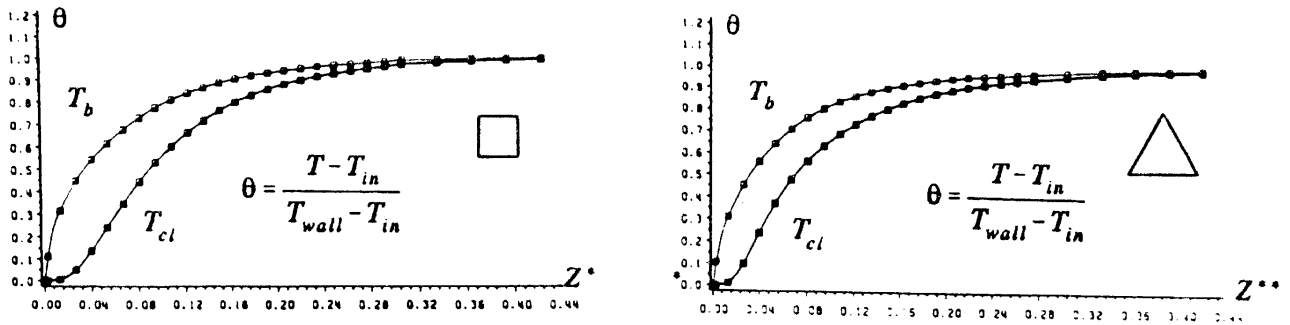
Figure 7. (a, b) D. L. temperature vs. D. L. axial distance, (square, triangular).
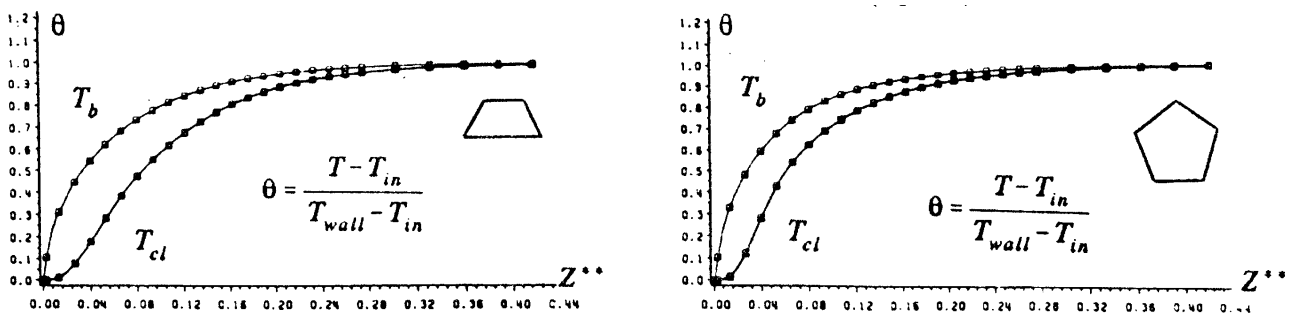

Figure 8. (a, b) D. L. temperature vs. D. L. axial distance, (trapezoidal, pentagonal).

or

$$\mathrm{Nu}_{m,T} = \frac{1}{4} G_z \ln\left(\frac{1}{\theta_b}\right) \qquad (30)$$

but

$$\theta_b = f(\mathrm{Pr}) \qquad (31)$$

therefore

$$\mathrm{Nu}_{m,T} = \frac{1}{4} G_z g(\mathrm{Pr}) \qquad (32)$$

or

$$\mathrm{Nu}_{m,T} = h(G_z, \mathrm{Pr}) \qquad (33)$$

The results of local and mean Nusselt numbers for ducts of different cross-sectional geometries are presented in Tables 6 and 7.

5. CONCLUSIONS

This paper shows the application of a non-orthogonal boundary fitted coordinate (BFC) procedure in the solution of 3D parabolized momentum and energy equations for various non-circular cross-sectional ducts. The thermal entrance region temperature profiles, thermal entry lengths, Nusselt number variations and limiting Nusselt number values are obtained for square, triangular, trapezoidal and pentagonal ducts. Experimental work is required in the entrance region of noncircular ducts to verify some of the results.

TABLE 6. $Nu_{z,T}$, Variations of Different Geometries.

G_x	Square	Triangular	Trapezoidal	Pentagonal
100	4.635	4.373	4.564	4.689
75	4.104	3.871	4.025	4.157
60	3.767	3.575	3.701	3.844
50	3.527	3.377	3.479	3.633
43	3.345	3.234	3.314	3.481
37	3.204	3.126	3.186	3.366
0	2.980	2.598	2.979	3.098

TABLE 7. $Nu_{m,T}$ Variations of Different Geometries.

G_x	Square	Triangular	Trapezoidal	Pentagonal
100	7.186	6.841	7.005	7.009
75	6.386	6.072	6.232	6.266
60	5.842	5.555	5.706	5.761
50	5.441	5.178	5.320	5.391
43	5.129	4.889	5.022	5.105
37	4.878	4.659	4.783	4.877
0	2.980	2.598	2.972	3.098

6. NOMENCLATURE

a	coefficient in the discretization equations
AR	aspect ratio
b	constant term in the discretization equations
C_p	specific heat
D. L.	dimensionless
D_h, DE	hydraulic diameter (or equivalent diameter)

$$DE = 4r_h = \frac{4 \times \text{flow area}}{\text{wetted perimeter}}$$

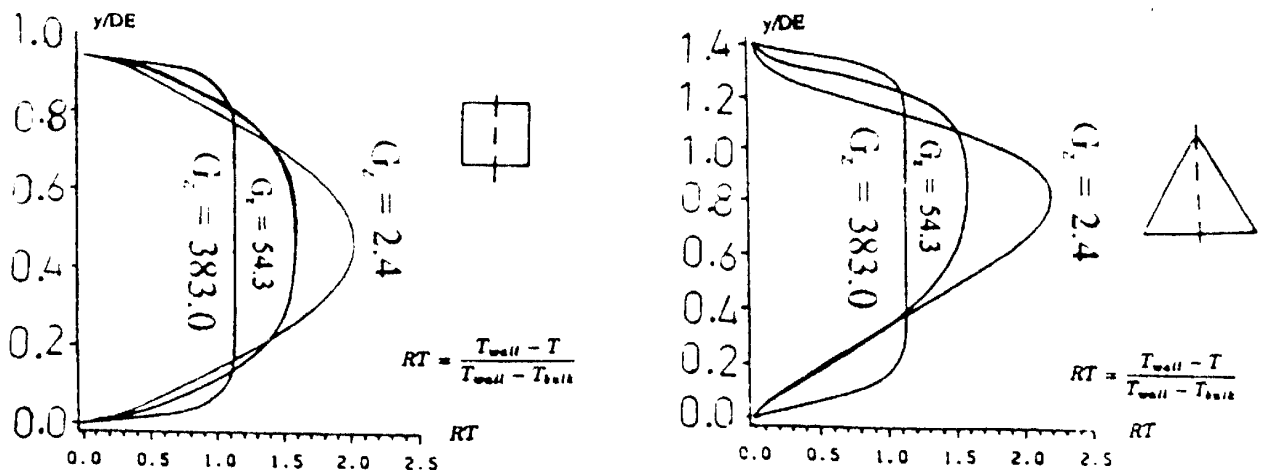|	
g	acceleration due to gravity
G_z	Greatz number ($G_z = \dfrac{1}{Z^{**}}$)
h	enthalpy ($h = C_P T$)
I	index of "ξ" axis in transformed plane
J	index of "η" axis in transformed plane
J	Jacobian of transformation
k	thermal conductivity
L1	maximum value of "I" index (on "ξ" axis)
M1	maximum value of "J" index (on "η" axis)
$Nu_{z,T}$	local Nusselt number
$Nu_{m,T}$	mean Nusselt number
Nu_T	limiting Nusselt number
P	total pressure (dynamic + hydrostatic)
P	dynamic pressure
$\overline{P}$	mean viscous pressure
Pr	Prandtl number ($Pr = \dfrac{C_P \mu}{k}$)
Pe	Peclet number ($Pe = Re \cdot Pr = \dfrac{\rho C_P D_h \overline{w}}{k}$)
q	heat flux
R	residual of discretization equation
R_e	Reynolds number ($Re = \dfrac{\rho (D_h) \overline{w}}{\mu}$)
T	temperature

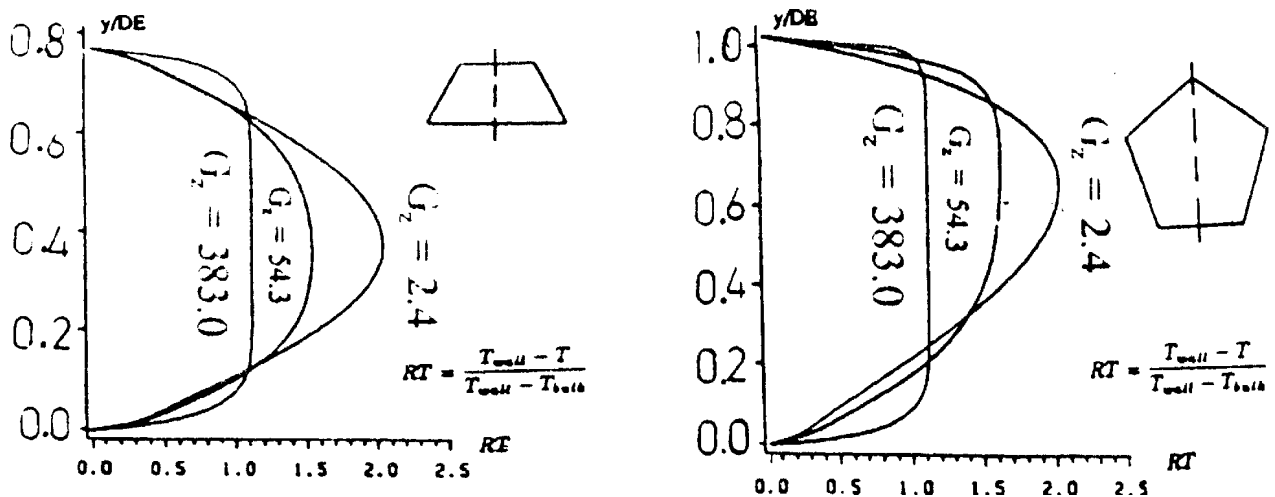**Figure 9**. (a, b) Development of the temperature profile, (square, triangular).

Figure 10. (a, b) Development of the temperature profile, (trapezoidal, pentagonal).

t_l	inlet temperature	$\overline{w}$	mean axial velocity
t_w	wall temperature	x, y, z	Cartesian coordinate system
u, v, w	velocity components in the Cartesian system	X	dimensionless axial distance
U, V, W	contravariant velocity components		
[v]	average axial velocity coefficients	Z^{**}	dimensionless axial-distance, $Z^{**} = \dfrac{z/D_h}{P_e}$
v	velocity field		

Greek Letters

α, β, γ transformation coefficients

ξ, η, σ axes of curvilinear coordinate

μ viscosity

ρ density

ρ_a arithmetic mean density

ϕ_v viscous dissipation function

τ_{ij} stress-tensor

Δ_{ij} rate of deformation tensor

θ dimensionless temperature, $\theta = \dfrac{t - t_w}{t_1 - t_w}$

ϕ a general dependent variable

Subscripts

nb   general neighbor grid point

Superscripts

^   refers to the transformed quantity

7. APPENDIX

Derivation of Local and Mean Nusselt Number

From Bird [11] (Page 423):

$$dQ = h_{loc}\left(\pi D dz\right)\left(T_o - T_b\right)$$
$$\rightarrow dQ = h_{loc} P dz\left(T_w - T_b\right) \tag{34}$$

in which P: perimeter, $T_o = T_w = T_{wall}$

$$dQ = \left(\frac{\pi D^2}{4}\right)\rho\, C_P\left[v\right]dT_b$$
$$\rightarrow dQ = A_c \rho C_P \overline{w}\, dT_b \tag{35}$$

in which A_c cross-sectional area

$$h_{loc} = \frac{A_c}{P}\left(C_P \mu\right)\left(\frac{\rho\overline{w}}{\mu}\right)\frac{dT_b}{\left(T_w - T_b\right)dz} \tag{36}$$

$$Nu_{loc} = \frac{h_{loc}\left(DE\right)}{k}$$
$$= \frac{A_c}{P}\left(\frac{C_P \mu}{k}\right)\left(\frac{\rho\overline{w}\left(DE\right)}{\mu}\right)\frac{dT_b}{\left(T_w - T_b\right)dz} \tag{37}$$

$$Nu_{loc} = \frac{A_c}{P}\left(Pr\right)\left(Re\right)\frac{dT_b}{\left(T_w - T_b\right)dz} \tag{38}$$

$$Nu_{loc} = \frac{A_c}{DE \cdot P}\frac{\dfrac{dT_b}{\left(T_w - T_1\right)}}{\dfrac{\left(T_w - T_b\right)}{\left(T_w - T_1\right)}}\frac{1}{\dfrac{dz}{\left(DE \cdot Re \cdot Pr\right)}} \tag{39}$$

$$\frac{dT_b}{T_w - T_1} = -\frac{d\left(T_w - T_b\right)}{T_w - T_1}$$
$$= -d\left(\frac{T_w - T_b}{T_w - T_l}\right) = -d\theta_b \tag{40}$$

in which

$$\theta_b = \frac{T_w - T_b}{T_w - T_1} \tag{41}$$

also

$$\frac{dz}{DE \cdot Re \cdot Pr} = d\left(\frac{z}{DE \cdot Pe}\right) = dZ^{**} \tag{42}$$

and from the definition $DE = 4 \dfrac{A}{P}$

one can write $\dfrac{Ac}{DE \cdot P} = \dfrac{1}{4}$

therefore

$$Nu_{loc} = -\frac{1}{4\theta_b} \frac{d\theta_b}{dZ^{**}} \tag{43}$$

$$\int_0^{Z^{**}} Nu_{loc} \cdot dZ^{**} = -\frac{1}{4} \int_1^{\theta_b} \frac{d\theta_b}{\theta_b} \tag{44}$$

$$Nu_{m,T} \cdot Z^{**} = -\frac{1}{4} \ln \theta_b \tag{45}$$

8. REFERENCES

1. Clark S. H. and Kays, W. N., "Laminar Flow Forced Convection in Rectangular Ducts", *Trans. ASME 75*, (1953), 859-866.
2. Han, L. S., "Laminar Heat Transfer in Rectangular Channels", *J. Heat Transfer, Trans. ASME Series C81*, (1959), 121-128.
3. Sparrow M. and Siegel, R., "A Variational Method for Fully Developed Laminar Heat Transfer in Ducts", *J. Heat Transfer, Trans. ASME Series C81*, (1959), 157-167.
4. Dennis, S. C. R., Mercer, A. McD. and Poots, G., "Forced Heat Convection in Laminar Flow through Rectangular Ducts", *Quart. Journal Appl. Math.*, Vol. 17, (1959), 285-297.
5. Savino, J. M. and Siegel, R., "Laminar Forced Convection in Rectangular Channels with Unequal Heat Addition on Adjacent Sides", *Int. Journal Heat Mass Transfer*, Vol. 7, (1964), 733-741.
6. Montgomery, S. R. and Wibulswas, P., "Laminar Flow Heat Transfer in Ducts of Rectangular Cross-Section", *ibid.*, Vol. 1, (1966).
7. Shah, R. K. and London, A. L., "Laminar Flow Forced Convection in Ducts", Academic Press, New York, (1978).
8. Lyczkowski, R. W., Solbrig, C. W. and Gidaspow, D., "Forced Convection Heat Transfer in Rectangular Ducts", *Nucl. Eng. and Design*, Vol. 67, (1981), 357-378.
9. Neti, S. and Eicbhorn, R., "Combined Hydrodynamic and Thermal Development in a Square Duct", *Num. Heat Transfer*, Vol. 6, (1983), 497-510.
10. Isazadeh, M. A., "Numerical Solution of Reacting Laminar Flow Heat and Mass Transfer in Ducts of Arbitrary Cross-Sections for Power-Law Fluid", Ph.D Thesis, McGill University, Montreal, Canada, (1993).
11. Bird, R. B., Steward, W. E. and Lightfoot, E. N., "Transport Phenomena", John Wiley and Sons, N. Y., (1960).
12. Allen, P. H. C., "Heat and Mass Transfer by Combined Forced and Natural Convection", The Institution of Mechanical Engineers, (1972).
13. Ostrach, S., "Laminar Natural-Convection Flow and Heat Transfer of Fluids with and without Heat Sources in Channels with Constant Wall Temperature", *NACA Technical Note 2863*, (1952).
14. Chu, W. H., "Development of a General Finite Difference Approximation for a General Domain", *Journal Cornp. Physics*, Vol. 8, (1971), 392-408.
15. Thompson, J. F., Thames, F. C., and Mastin, C. W., "Boundary-Fitted Curvilinear Coordinate Systems for Solution of Partial Differential Equations on Fields Containing any Number of Arbitrary Two-Dimensional Bodies", *Report CR-2729, NASA Langley Research Centre*, (1977).
16. Patankar, S. V., and Spalding, D. B., "A Calculation Procedure for Heat, Mass and Momentum Transfer in Three-Dimensional Parabolic Flows", *Int. J. Heat Mass Transfer*, Vol. 15, (1972), 1787-1806.
17. Patankar, S. V., "Numerical Heat Transfer and Fluid Flow", Hemisphere Publishing Corporation, N. Y., (1980).
18. Raithby, C. D. and Schneider, G. E., "Numerical Solution of Problems in Incompressible Fluid Flow: Treatment of the Velocity-Pressure Coupling", *Numerical Heat Transfer*, Vol. 2, (1979), 417-440.
19. Caretto, L. S., Curr, R. M. and Spalding, D. B., *Comp. Meth. Appl. Mech. and Engr.*, Vol. 1, No. 39, (1973).
20. Briley, W. R., "Numerical Method for Predicting Three Dimensional Steady Viscous Flow in Ducts", *Journal Comp. Physics*, Vol. 14, (1974), 8-28.
21. Hadjisophocleous, G. V., Sousa, A. C. M. and Venart, J. E. S., "Prediction of Transient Natural Convection in Enclosure of Arbitrary Geometry Using a No Orthogonal Numerical Model", *Numerical Heat Transfer*, Vol. 13, (1988), 373-392.
22. Shyy, W., Tong, S. S. and Correa, S. M., "Numerical Recirculating Flow Calculation Using a Body-Fitted

Coordinate System", ***Numerical Heat Transfer***, Vol. 8, (1985), 99-113.

23. Braaten, M. and Shyy, W., "A Study of Recirculating Flow Computation Using Body-Fitted Coordinates: Conszstency Aspects and Mesh Skewness", ***Numerical Heat Transfer***, Vol. 9, (1988), 559-574.

24. Maliska, C. R. and Raithby, G. D., "A Method for Computing Three-Dimensional Flows Using Non-Orthogonal Boundary-Fitted Coordinates, ***Int. J. for Numerical Methods in Fluids***, Vol. 4, (1984), 519-537.

25. Bejan, A., "Convection Heat Transfer", Prentice Hall, N. J., (1984).

26. Kays, W. M. and Crawford, M. E. "Convective Heat and Mass Transfer", Second Ed., McGraw Hill, N. Y., (1980).

27. Chandrupatla, R. and Sastri, V. M. K., "Laminar Forced Convection Heat Transfer of a Non-Newtonian Fluid in a Square Duct", ***Int. Journal Heat Mass Transfer***, Vol. 20, (1977), 1315-1324.

28. Wibulswas, P., "Laminar Flow Heat Transfer in Non-Circular Ducts", Ph. D. Thesis, London University, London, (1966).